Dynamic heat transfer characteristics of ice storage in smooth-tube and corrugated-tube heat exchangers

Chengjun Li [a], Juan Hou [a], Yaran Wang [a,*], Shen Wei [b], Pengkun Zhou [a], Zhihao He [a], Yeming Wang [a], Huan Zhang [a], Shijun You [a]

[a] School of Environmental Science and Engineering, Tianjin University, Tianjin 300350, PR China

[b] The Bartlett School of Construction and Project Management, University College London (UCL), 1-19 Torrington Place, London WC1E 7HB, United Kingdom

[*] Corresponding author. E-mail addresses: yaran_wang@tju.edu.cn

Abstract

The ice storage system is one of the most promising techniques for flexibility enhancement of building cooling load. In this paper, the performances of smooth-tube and corrugated-tube heat exchangers for ice storage are compared by experiments and numerical simulation. The heat transfer process of the ice storage and melting within the heat exchangers is numerically analyzed used Python. The fast one-dimensional numerical model is verified by the experimental results. The temperature variation of the heat transfer fluid (HTF) in the corrugated tube is analyzed and compared with that in the smooth tube. The results show that under the same conditions, the ice storage duration of the corrugated tube is shortened by 25% and the melting duration is shortened by 16% compared with those of the smooth tube. During the ice storage process, the temperature difference between the inlet and outlet of the heat transfer fluid in the corrugated tube is 0.4 °C less than that of the smooth tube on average. The temperature change rate is 30% faster than that of the smooth tube. During the melting process, the temperature difference between the inlet and outlet of the heat transfer fluid in the corrugated tube is 0.1 ℃ higher than that of the smooth tube on average, and the temperature change rate of corrugated-tube heat exchanger is 2.5 times and 9 times faster than that of the smooth tube during the ice-storage and melting process. The corrugated-tube heat exchanger has superior performances in ice storage system in the comparison with the smooth-tube heat exchanger.

Keywords: Ice storage; Smooth tube; Corrugated tube; Prediction model

1. Introduction

The ice storage system is one of the most promising techniques for flexibility enhancement of building cooling load [1]. The inner melting ice storage tank is a widely adopted technique for cold storage air conditioning [2]. Its ice storage tube is placed in the ice storage tank. The low-temperature glycol solution flows within the tube, and the water freezes outside the tube.

While due to the low heat transfer coefficient of ice, the thermal resistance between the refrigeration medium and water increases with the thickness of ice. This heat transfer characteristic hinders the application of ice storage technology [3]. Therefore, many experiments [4, 5] and studies [6, 7] focus on enhancement of the heat transfer of ice storage systems. Heat transfer enhancement techniques can be divided into active and passive measures. The active measure requires mechanical assistance or electrostatic field, while the passive one does not require any external power supply [8, 9]. The passive measure can be summarized into four categories [10], including enlargement of the heat transfer area [3, 10], improvement of the thermal conductivity [11], using the PCM microencapsulation [12] and adding the metal foam [13, 14]. Considering the commercial cost and scheduling performance, the most commonly used measures are mainly enlargement of the heat transfer area and improvement of the thermal conductivity, including inserting fins [15] and adopting the corrugated-tube inserting fins. [16, 17].

Many studies show that the corrugated-tube heat exchangers are attracting more and more attention. The anti-scaling performance and thermal compensation of the corrugated-tube heat exchangers are stronger than those of the smooth-tube heat exchangers [18,19]. Therefore, the corrugated-tube heat exchangers are widely used in industry and living. Many experiments have investigated different types of corrugated tubes. Hu et al. [20] investigated and compared the flow and heat transfer characteristics of three corrugated tubes (transversely corrugated tube, helically corrugated tube [21] and outward corrugated tube) by combining experimental and numerical methods. They concluded that the corrugation could disrupt the boundary layer development, strengthen the turbulent mixing, reduce the temperature gradient in the boundary layer, and improve the synergy between the velocity field and the heat flux field, thus enhancing the heat transfer. Yang et al. [22] studied the turbulent friction and heat transfer characteristics of four spirally corrugated tubes with various geometrical parameters. The study concluded that the thermal performances of these tubes are superior compared to the smooth tubes. Peng et al. [23] conducted an investigation and optimization of heat transfer performance of spirally corrugated tubes using the Taguchi method. The study concluded that the corrugation depth and spacing had major effects on the heat transfer. A larger corrugation depth and smaller corrugation spacing could improve heat transfer performance. Navickaite et al. [9] investigated a comparison of heat transfer performance of double corrugated tubes and smooth tubes for laminar flow conditions. The study concluded that the novel geometry of corrugated tube affects the fluid by disturbing thermal boundary layers and modifying the flow profile compared to the smooth tubes as well as by increasing the area of the inner surface of the tube. Corcoles et al. [24] conducted a 3-D numerical simulation under turbulent regime of the flow pattern and heat transfer process in a double pipe heat exchanger at counter flow comparing several types of inner spirally corrugated tubes. The study concluded that the heat transfer rate, effectiveness and number of thermal units obtained in the corrugated cases increased in comparison to the smooth tube.

In previous studies, most researches focused on the inner corrugated tubes, such as the transversely corrugated tube and the helically corrugated tube. Chen et al. [25] investigated the heat transfer performance and flow characteristics of turbulent flow in asymmetrical corrugated tubes by experiments and numerical simulation. The study concluded that compared with the tube side of the asymmetrical corrugated tubes, the *Nu* and the performance evaluation criterion of shell side in the asymmetrical corrugated tubes is more obvious. While few researches focused on the heat transfer performance of the outward symmetrical corrugated-tube heat exchanger applied to ice storage. In this paper, the heat transfer performances of the smooth-tube and symmetrical corrugated-tube heat exchangers are investigated and compared by the experiment and numerical simulation. The numerical simulation simplify the mathematical model and analyze the transient temperature distribution fast during the ice-storage and melting process, which aims to optimize and adjust the operation stage of the ice storage project. The temperature of the corresponding positions of the two heat exchangers is compared to verify the enhancement performance of the corrugated-tube heat exchanger during the ice storage and melting process. In the paper, the comparative experiment of the smooth-tube heat exchanger and corrugated-tube heat exchanger is studied firstly. Then the one-dimensional mathematical model is established and numerically analyzed by Python. Finally, it is concluded that corrugated-tube heat exchanger has the superior heat transfer performances in comparison with the smooth-tube heat exchanger by comparing the ice-storage and melting rate and temperature distribution characteristics.

2. Experimental study

The ice storage system is equipped with the smooth-tube and corrugated-tube ice storage tank for comparative experiments. The air source heat pump chiller (ASHP) is used for refrigerating the heat transfer fluid. Ethylene glycol solution with mass fraction of 25% within the smooth-tube and corrugated-tube heat exchangers is used as the heat transfer fluid (HTF) to exchange the cold with the phase change material (PCM) outside the tube. The temperature distribution of HTF and PCM is monitored and recorded in real time.

2.1. Experimental system

The experimental system of smooth-tube and corrugated-tube heat exchangers is shown in Fig. 1. The schematic structural diagrams of the two heat exchangers are shown in Fig. 2 and Fig. 3, respectively.

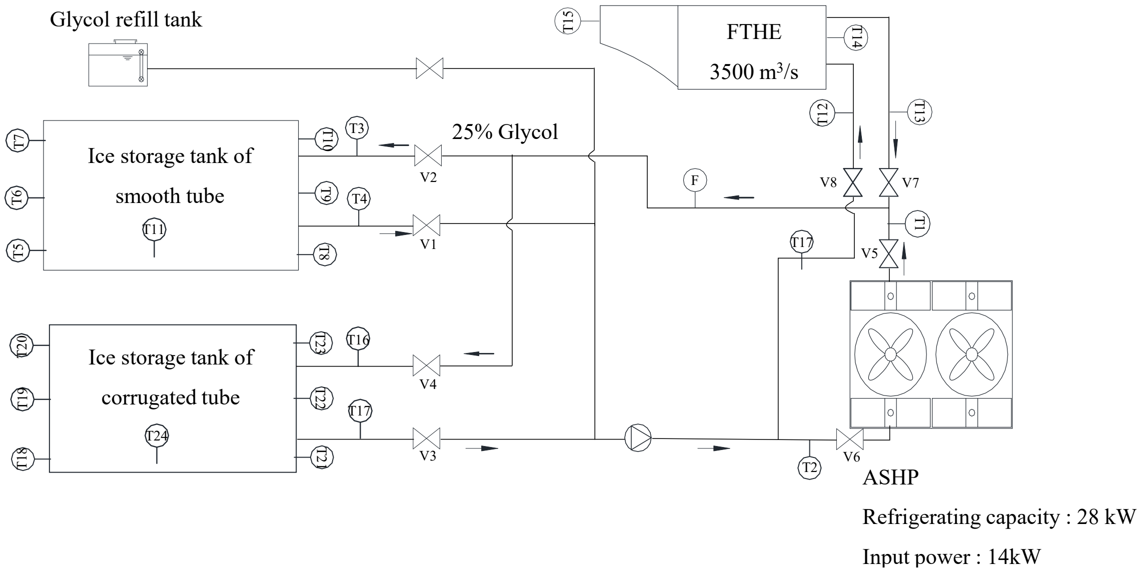

Fig. 1. Experimental system of ice storage and melting

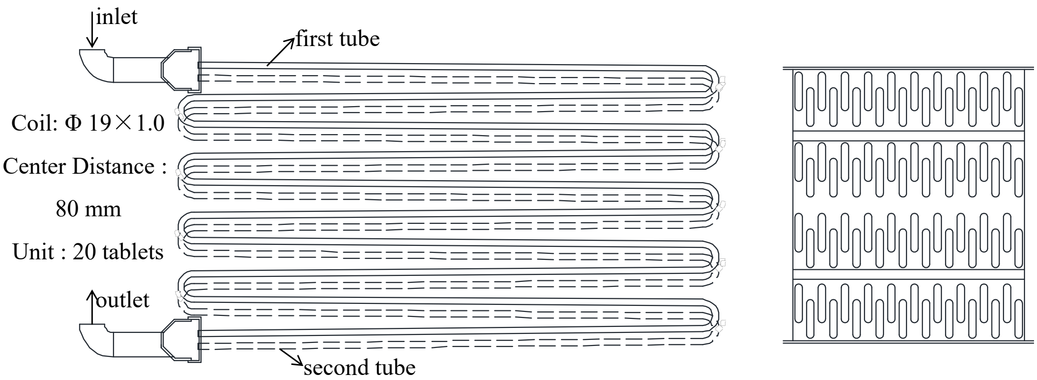

(a) Front view (b) Side view

Fig. 2. Structural diagram of smooth tubes

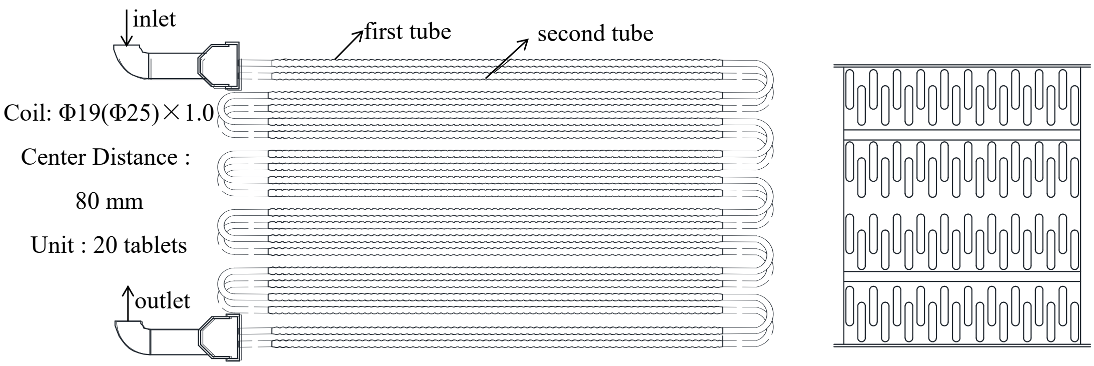

(a) Front view (b) Side view

Fig. 3. Structural diagram of corrugated tubes

The temperatures of HTF have been measured with thermal resistances PT100. The position of resistance thermometer sensors is shown in Fig.1. The location description of each sensor is shown in Table 1.

Table 1 Sensor location

Sensors	Measurement parameters
T1、T2	Supply and return water temperature of the ASHP
T3、T4	Inlet and outlet glycol temperature of the ice-storage tank with smooth tubes
T5、T8	Outlet glycol temperature of two smooth tubes
T6、T9	Glycol temperature at the medial positions of two smooth tubes
T7、T10	Inlet glycol temperature of two smooth tubes
T11	Water temperature of the ice-storage tank with smooth tubes
T12、T13	Inlet and outlet glycol temperature of the FTHE
T14、T15	Inlet and outlet air temperature of the FTHE
T16、T17	Inlet and outlet glycol temperature of ice storage tank with corrugated tubes
T18、T21	Outlet glycol temperature of two corrugated tubes
T19、T22	Glycol temperature at the medial positions of two corrugated tubes
T20、T23	Inlet glycol temperature of two corrugated tubes
T24	Water temperature of the ice-storage tank with corrugated tubes

2.2. Experimental process

2.2.1. Ice-storage experiment

The ice storage process of the ice-storage tank requires supply temperatures of the HTF below 0 ℃, which is achieved by providing chilled glycol from the ASHP to the heat exchangers. During the ice storage process, the low-temperature glycol solution enters the smooth-tube heat exchanger and corrugated-tube heat exchanger to lower the temperature of the water outside the tubes by heat exchange.

The ice storage processes of smooth-tube and corrugated-tube heat exchangers is transformed by opening and closing different valves. The conversion of valves is shown in Table 2. During the smooth-tube ice storage experiment, the valve 1, 2, 5 and 6 are opened and other valves are closed. During the corrugated-tube ice storage experiment, the valve 3, 4, 5, 6 are opened and other valves are closed. The installation is fully monitored by means of a datalogger with a recording interval of 1 min.

Table 2 Experimental conversion during the ice storage process

Valves	V1	V2	V3	V4	V5	V6	V7	V8
smooth tube	opened	opened	closed	closed	opened	opened	closed	closed
corrugated tube	closed	closed	opened	opened	opened	opened	closed	closed

Since it is difficult to observe the situation inside the ice-storage tank, the level gauge installed outside the ice-storage tank is used for observing the variation of PCM volume. During the ice storage process of the smooth-tube heat exchanger, the ice-storage experiment stops when it is observed that there is no gap between the ice layer outside the tubes. The rising height (1.1 cm) of liquid level is marked on the level gauge. In order to ensure that the ice storage capacities of the two ice-storage tanks are the same, the rising height of the liquid level should be identical. When the liquid level rises to the same height in the corrugated-tube experiment as in the smooth-tube experiment, the ice-storage experiment of the corrugated-tube heat exchanger stops.

2.2.2. Melting experiment

The melting process of the ice-storage tank requires supply temperatures of the HTF above 0 °C. This is achieved using the outdoor air which heats the HTF by means of the finned tube heat exchanger (FTHE). During the melting process, outdoor air is blown into the FTHE to exchange heat with the low-temperature glycol solution from the smooth-tube and corrugated-tube heat exchangers. Then the glycol solution with increased temperature enters the smooth-tube and corrugated-tube exchangers to exchange heat with the water outside the tubes, and the low-temperature air is blown out of the room.

The conversion of smooth-tube and corrugated-tube heat exchangers experiment is shown in Table 3. During the smooth-tube melting experiment, the valve 1, 2, 7 and 8 are opened and other valves are closed. During the corrugated-tube melting experiment, the valve 3, 4, 7, 8 are opened and other valves are closed.

Table 3 Experimental conversion during the melting process

Valves	V1	V2	V3	V4	V5	V6	V7	V8
smooth tube	opened	opened	closed	closed	closed	closed	opened	opened
corrugated tube	closed	closed	opened	opened	closed	closed	opened	opened

During the melting process, the experiment stops when the liquid level decreases to initial position before the ice-storage experiment. The flow direction of HTF is from top to bottom. There are greater turbulence intensity and larger temperature difference of water in the upper part of the tank. Therefore, the ice layer above melts first. The PCM is presented in the form of ice-water mixture. During the melting process, floating ice floats on the surface of water when the ice layer outside the tubes is broken.

2.3. Uncertainty analysis

A theoretical calculation of the thermal resistances shows that the insulation resistance is much higher than the rest of thermal resistances. Thus, the thermal-sensors which are attached to the tube wall practically measure the temperature of the HTF inside the tube [26]. The uncertainty associated with each measurement value is summarized in Table 4.

Table 4 Accuracy of the measurement equipment

Equipment	Model	Range	Accuracy
Thermal resistances (temperature of the HTF)	PT100	-30 ℃ to 80 ℃	± 0.2 ℃
Flow meter (mass flow rate)	FS01A	2.3 - 23 m^3/h	± 0.0115 m^3/h
Datalogger: RTD input	GL840	-	± 0.6 ℃

3. Numerical modeling

3.1. Physical model

The geometric model of the ice-storage tube is shown in Fig. 4.

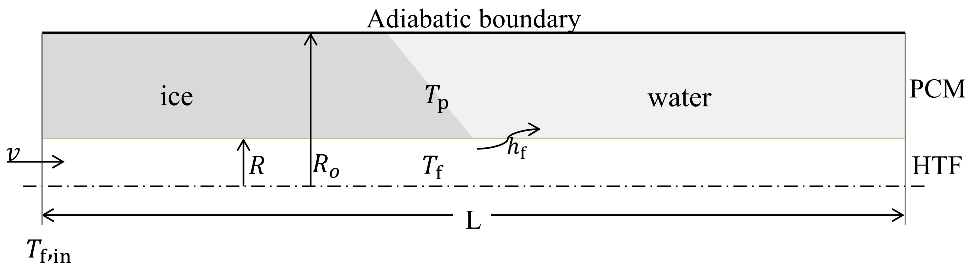

Fig. 4. Physical model diagram of ice storage

The HTF flows within the tube and exchanges heat with PCM outside the tube. During the ice storage process, the heat is transferred from the high-temperature PCM to the low-temperature HTF. During the melting process, the heat is transferred from the HTF to the PCM and stored in the PCM. The length of the computational domain is 16.5 m and the diameter of the tube is 20 mm.

The one-dimensional numerical model of the heat transfer characteristics of the smooth-tube and corrugated-tube heat exchangers is developed, which aims to simulate the temperature distribution fast during the ice-storage and melting process . The model is based on the following assumptions:

(1) Axial heat conduction and viscous dissipation of HTF are negligible;

(2) The temperature distributions of the HTF and PCM are uniform at the initial state;

(3) The thermal resistance and fouling factors of the tube wall are negligible;

(4) Heat loss to the surroundings is negligible;

(5) Natural convection and radiation heat transfer of water is negligible.

3.2. Mathematical model

The mathematical model of the heat exchangers is established based on the rectangular coordinate system considering the thermal characteristics and boundary conditions of the HTF and the PCM. The tube radius is much smaller than the length of the tube, so one-dimensional energy balance equation is adopted [27].

$$\frac{\partial(\rho T)}{\partial \tau} = div\left(\frac{\lambda}{c} \cdot gradT\right) + S_h \tag{1}$$

$$\frac{\partial(\rho T)}{\partial \tau} + div(\rho \vec{v} T) = div\left(\frac{\lambda}{c} \cdot gradT\right) + S_T \tag{2}$$

The enthalpy method is used to solve the moving boundary problem of the phase change process. If the enthalpy of the ice at 0 ℃ is 0 J/kg, the enthalpy of the water at 0 °C is 334000 J/kg. The enthalpy equation of the PCM is calculated as [28]:

$$\frac{\partial(\rho H)}{\partial \tau} = div(\lambda \cdot gradT) + S_h \tag{3}$$

where τ (s) is the interval time, T (°C) is the temperature, H (J/kg) is the enthalpy, and S_h、 S_T (W/m^2) is the source term.

The solid mass fraction is used to describe the ice-water mixing zone. In the full solid zone, the mass fraction fm = 1. When it is the liquid phase, fm tends to be zero. The mass fraction is computed as:

$$fm = \begin{cases} 1 & H \le H_{\mathrm{ice}} \\ 1 - \dfrac{H}{H_{\mathrm{water}}} & H_{\mathrm{ice}} < H < H_{\mathrm{water}} \\ 0 & H \ge H_{\mathrm{water}} \end{cases} \tag{4}$$

where H_{ice} is the enthalpy of solid phase at 0 ℃ and H_{water} is the enthalpy of liquid phase at 0 ℃.

The energy balance equations can be discretized based on the control volume integral method and the implicit difference method. The energy balance equation of HTF is:

$$\frac{\rho_{\mathrm{f}} c_{\mathrm{f}} \pi R^2 \Delta x}{\Delta \tau}\left(T_{\mathrm{f},i}^{n+1} - T_{\mathrm{f},i}^{n}\right) = \pi R^2 \cdot \frac{2\lambda_f}{\Delta x}\left(T_{\mathrm{f},i-1}^{n+1} - 2T_{\mathrm{f},i}^{n+1} + T_{\mathrm{f},i+1}^{n+1}\right) + \frac{\rho_{\mathrm{f}} c_{\mathrm{f}} \pi R^2 v}{2}\left(T_{\mathrm{f},i-1}^{n+1} - T_{\mathrm{f},i+1}^{n+1}\right)$$
$$+ 2\pi R \Delta x h_{\mathrm{f}}\left(T_{\mathrm{p},i}^{n+1} - T_{\mathrm{p},i}^{n+1}\right) \tag{5}$$

The energy balance equation of PCM is:

$$\frac{\rho_{\mathrm{p}i} \Delta x}{\Delta \tau}\left(H_i^{n+1} - H_i^{n}\right) = \left[\frac{2\lambda_{\mathrm{p},i-1}^{n+1}\lambda_{\mathrm{p},i}^{n+1}}{\lambda_{\mathrm{p},i-1}^{n+1} + \lambda_{\mathrm{p},i}^{n+1}}\left(\frac{T_{\mathrm{p},i-1}^{n+1} - T_{\mathrm{p},i}^{n+1}}{\Delta x^2}\right) + \frac{2\lambda_{\mathrm{p},i+1}^{n+1}\lambda_{\mathrm{p},i}^{n+1}}{\lambda_{\mathrm{p},i+1}^{n+1} + \lambda_{\mathrm{p},i}^{n+1}}\left(\frac{T_{\mathrm{p},i+1}^{n+1} - T_{\mathrm{p},i}^{n+1}}{\Delta x^2}\right)\right]$$
$$+ \frac{2Rh_{\mathrm{f}}}{R_o^{\,2} - R^2}\left(T_{\mathrm{f},i}^{n+1} - T_{\mathrm{p},i}^{n+1}\right) \tag{6}$$

where ρ_{f} (kg/m^3) is the density of the HTF, c_{f} [J/(kg·℃)] is the specific heat capacity of the HTF, λ_{f} [W/(m·℃)] is the thermal conductivity of the HTF, T_{f} (℃) is the temperature of the HTF, R (m) is the radius of the HTF, R_o (m) is the radius of the PCM, v (m/s) is the flow rate of the HTF, h_{f} [W/(m^2·℃)] is the convection heat transfer coefficient between the HTF and the PCM, as can be inferred from Eq. (7) [29, 30]:

$$h_{\mathrm{f}} = \frac{Nu_{\mathrm{f}} \cdot \lambda_{\mathrm{f}}}{2R} \tag{7}$$

Smooth tube

$$Nu_{\mathrm{f}} = 0.012\left(\mathrm{Re}^{0.87} - 280\right)\mathrm{Pr_f}^{0.4}[1 + (\frac{2R}{L})^{\frac{2}{3}}]\left(\frac{\mathrm{Pr_f}}{\mathrm{Pr_p}}\right)^{0.11} \tag{8}$$

Corrugated tube

$$Nu_{\mathrm{f}} = 0.07895\,\mathrm{Re}^{0.8134} \cdot \mathrm{Pr_f}^{0.4} \tag{9}$$

where $\mathrm{Pr_f}$ and $\mathrm{Pr_p}$ are the Prandtl number at HTF temperature and PCM temperature, respectively, L is the length of the computational domain.

The relationship between the temperature and enthalpy of the PCM is defined as:

$$T_{\mathrm{p}} = \begin{cases} \dfrac{H}{c} & H \le H_{\mathrm{ice}} \\ 0 & H_{\mathrm{ice}} < H < H_{\mathrm{water}} \\ \dfrac{H - H_{\mathrm{water}}}{c} & H \ge H_{\mathrm{water}} \end{cases} \tag{10}$$

The physical properties of the PCM can be expressed as follows [3],

$$c_{\mathrm{p}} = 2090\,fm + 4200(1 - fm) \tag{11}$$

$$\lambda_{\mathrm{p}} = 2.22\,fm + 0.55(1 - fm) \tag{12}$$

$$\rho_{\mathrm{p}} = \frac{1000 \times 998}{1000\,fm + 998(1 - fm)} \tag{13}$$

where c_{p} [J/(kg·°C)] is the specific heat capacity of the PCM, λ_{p} [W/(m·°C)] is the thermal conductivity of the PCM, ρ_{p} (kg/m^3) is the density of the PCM, and T_{p} (°C) is the temperature of the PCM.

At the initial time, the temperatures of the HTF are equal to them of the PCM. The inlet temperatures of both HTF and PCM are defined as T_{in}. Assuming the first-type and second-type boundary conditions, the initial and boundary conditions are defined as:

$$\tau = 0: \quad T_{\mathrm{f}} = T_{\mathrm{p}}$$

$$x = 0: \quad T_{\mathrm{f}} = T_{\mathrm{p}} = T_{\mathrm{in}}$$

$$x = L: \quad \frac{\partial T_{\mathrm{f}}}{\partial x} = \frac{\partial T_{\mathrm{p}}}{\partial x} = 0$$

3.3. Numerical solution

In this study, the process of ice storage and melting is modeled and numerically solved by Python. The computational domain is divided by uniform rectangular grids. To ensure the accuracy of numerical results, a grid independence test is conducted. Four different grid systems are selected as examples, including the cases with the number of grids (i.e. N) of 33, 55, 165 and 275, respectively. The total heat transfer of the HTF during the ice-storage process for cases with different grid systems is shown in Fig. 5. As demonstrated in the figure, the predicted dynamic response of total heat transfer for case with N = 165 agrees well with that with N = 330. Therefore, considering the calculation cost and independence test results, the number of grids of 165 (grid size is determined as 0.1 m) is selected in the present work.

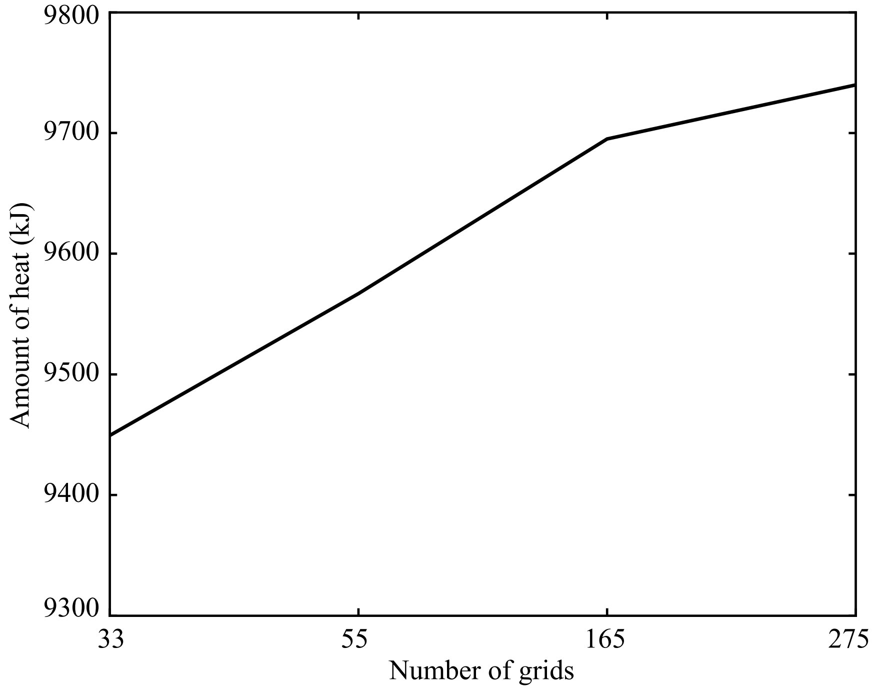

(a) Total heat transfer of smooth-tube heat exchanger during the ice-storage process

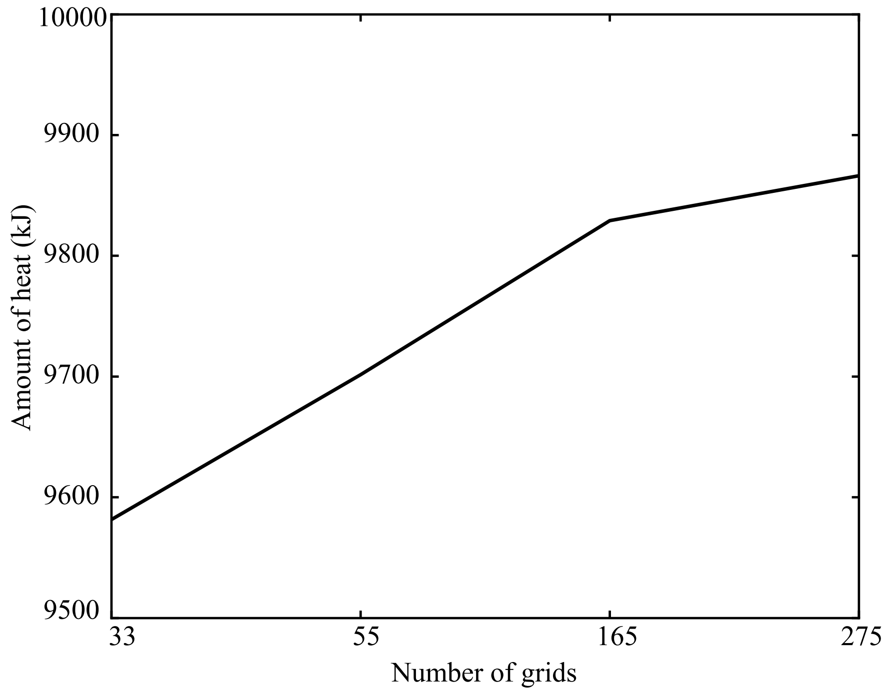

(b) Total heat transfer of corrugated-tube heat exchanger during the ice-storage process

Fig. 5. Grid independence test

There are two unknown variables H and T in Eq. (6). It cannot be directly solved. It is necessary to convert the equation into a form of only one variable H. Firstly, the initial temperature ($T_{f,i}$ and $T_{p,i}$) of each node are given by the initial conditions. According to Eq. (10), the Eq. (6) is expressed as the expression of H_p in order to unify the equation into the form of only one variable H. Secondly, the Eq. (5) and enthalpy equation Eq. (6) are simultaneously solved based on the two-variable TDMA method to figure out new temperatures ($T_{f,i}$) of the HTF and new enthalpy values (H_i) of the PCM for each node. If the new values and initial-time values satisfies the convergence conditions, the new values are the final solution of this time layer. Then, $T_{p,i}$ is calculated from H_i according to Eq. (10). If the convergence conditions are not satisfied, the new values ($T_{f,i}$ and H_i) are brought into Eq. (5) and Eq. (6). The above procedures are iterated until the results are convergent. Lastly, final values of this time layer are taken as initial values of the next time layer. The above procedures are iterated to compute temperatures of each time layer. The numerical algorithm process is shown in Fig. 6.

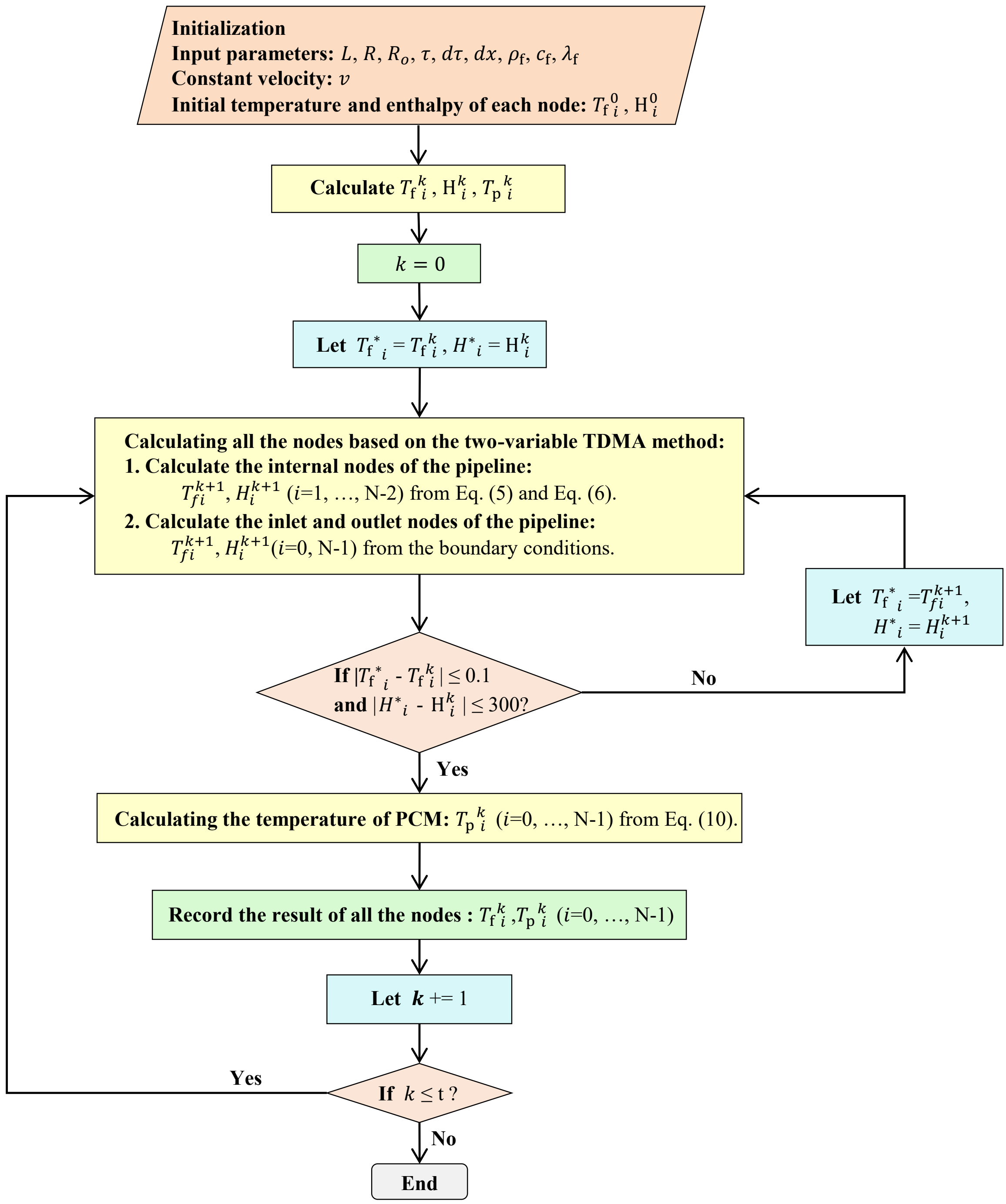

Fig. 6. Numerical simulation program

4. Results and Discussion

4.1. Experimental results

4.1.1 Ice storage process

The temperature measurements in the inlet and outlet of the HTF within the corrugated-tube and smooth-tube heat exchangers are shown in Fig. 7.

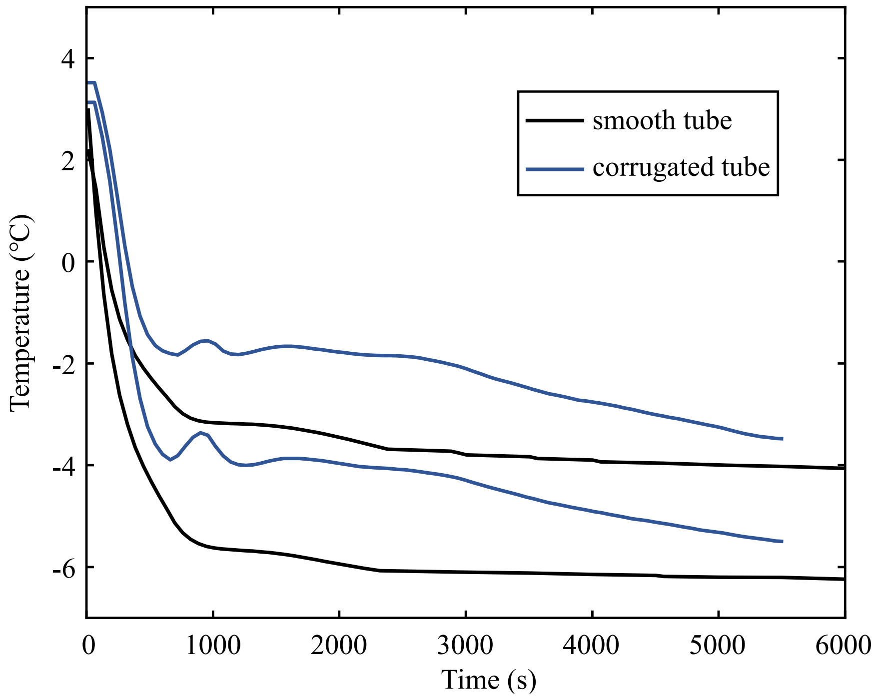

Fig. 7. Inlet and outlet temperature of HTF within the two heat exchangers versus time during the ice storage process

The ice-storage duration of the smooth-tube heat exchanger is 7197 s. The ice-storage duration of the corrugated-tube heat exchanger is 5402 s, which is shortened by 25% compared with that of the traditional smooth-tube heat exchanger. The inlet temperature of smooth-tube heat exchanger rapidly declines from 3 °C to -5.7 °C during the first 12.51% of the smooth-tube ice storage duration, and is stable between -5.7 °C and -6.1 °C during the following period. For the corrugated-tube heat exchanger, the inlet temperature rapidly declines from 3 °C to -4 °C during the first 12.96% of the corrugated-tube ice storage duration, and then slowly decreases from

-4 °C to -5.5 °C. This is because that the HTF temperature is close to the indoor temperature at the initial stage of the ice storage process. The HTF temperature decreases rapidly when the ASHP runs and remains stable when the inlet temperature satisfies the temperature requirements for the experiment. The outlet temperature of smooth-tube heat exchanger rapidly declines from 3 °C to -3 °C during water sensible heat storage period, and slowly decreases from -3 °C to -3.5 °C during ice latent heat storage period. For the corrugated-tube exchanger, the outlet temperature rapidly declines from 3 °C to -1.7 °C and slowly decreases from -1.7 °C to -3.2 °C.

The average drop rate of the outlet temperature of the corrugated-tube heat exchanger is 4.1 °C/h, which is 19.5% faster than that of the smooth-tube heat exchanger. So the PCM of the corrugated-tube heat exchanger reaches the solidification point faster.

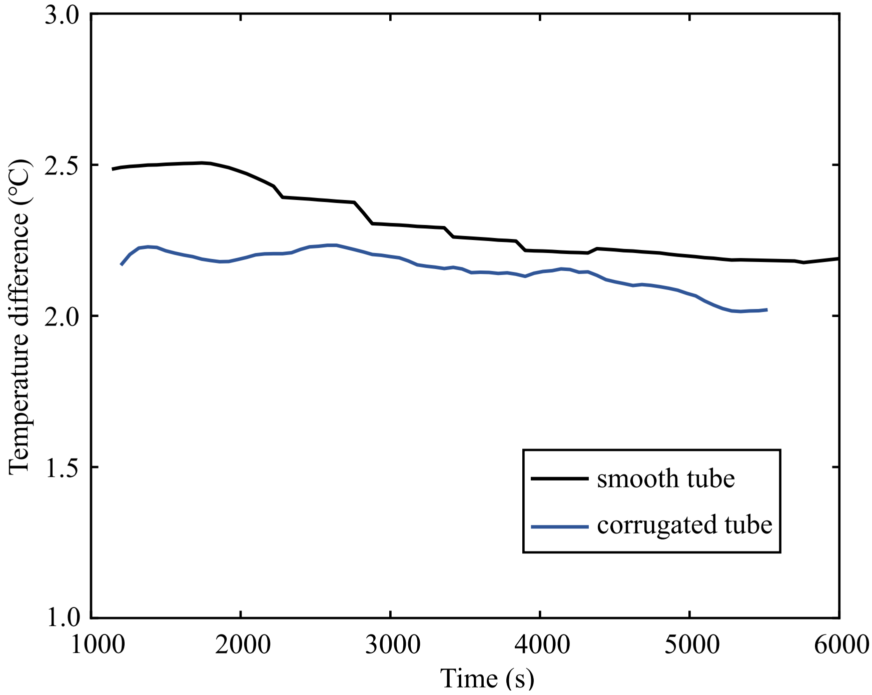

Fig. 8. Temperature differences of the two heat exchangers versus time during the ice storage process

As shown in Figure 8, the difference in temperature of the two heat exchangers between inlet and outlet decreases with the ice-storage time. In addition, it is also seen from Fig. 8 that the temperature difference between the inlet and outlet of the corrugated-tube heat exchanger is 0.4 ℃ less than that of the smooth-tube heat exchanger during ice latent heat storage period. This can be indicated that the heat exchange between HTF and PCM of corrugated-tube heat exchanger is more sufficient and the heat transfer performance of corrugated-tube heat exchanger are superior compared with the smooth-tube heat exchanger. This is because that cyclic changes of the surface area of the corrugated tube change the fluid flow pattern and strengthen the fluid mixing. The corrugations disrupt the development of the thermal boundary layer and improve the convective heat transfer performances.

4.1.2 Melting process

Fig. 9 shows the inlet and outlet HTF temperature of the corrugated-tube and smooth-tube heat exchangers.

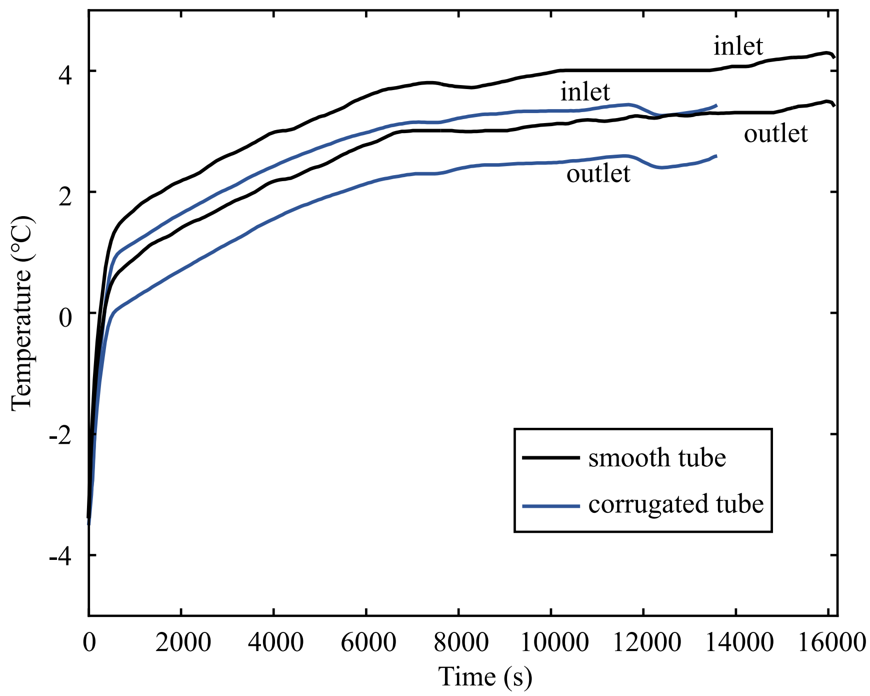

Fig. 9. Inlet and outlet temperature of HTF within the two heat exchangers versus time during the melting process

The melting duration of the smooth-tube heat exchanger is 16140 s. The melting duration of the corrugated-tube heat exchangers is 13560 s, which is shortened by about 43 minutes compared with that of the smooth-tube heat exchangers. The inlet temperature of smooth-tube heat exchanger increases rapidly from -3.5 ℃ to 1.5 ℃ during the first 3.1% of the smooth-tube duration, and is stable between 1.5 ℃ and 4 ℃ during the following period from 500s to 16140s. For the corrugated-tube heat exchanger, the inlet temperature increases rapidly from -3.5 ℃ to 1 ℃ during the first 4.4% of the corrugated-tube duration, and then slowly increases from 1 ℃ to 3 ℃. This is because that the temperature of melting in the ice-storage tank is relatively low during the initial melting period, which increases rapidly when the FTHE runs. When the HTF temperature satisfies the temperature requirements of the experiment, it keeps stable.

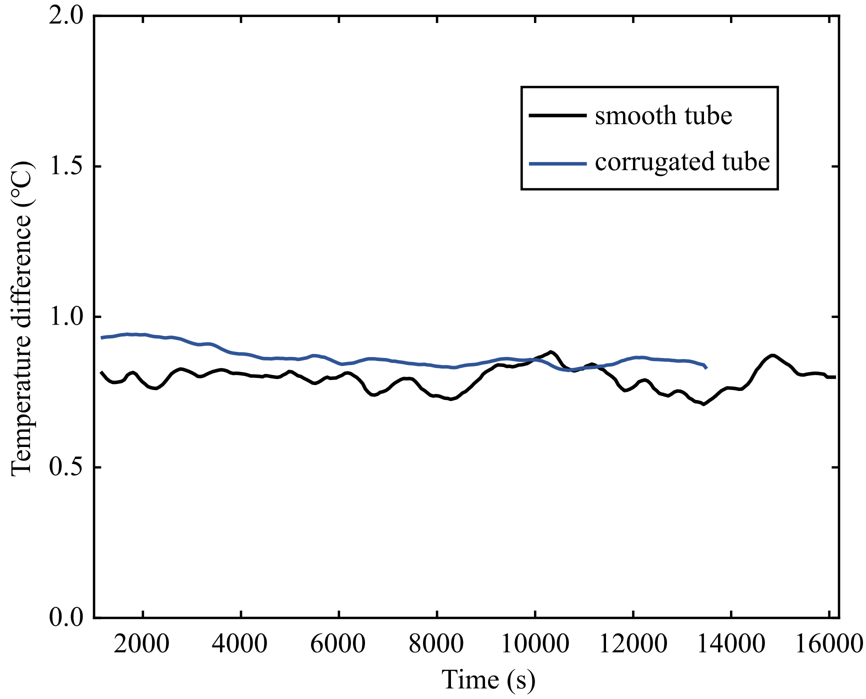

Fig. 10. Temperature differences of the two heat exchangers versus time during the melting process

As shown in Fig. 10, the average temperature difference between the inlet and outlet of smooth-tube heat exchanger is 0.75 °C and that of corrugated-tube HTF is 0.85 °C. The average rising rate of the outlet temperature of smooth-tube and corrugated-tube heat exchangers is 1.56 °C/h and 1.73 °C/h, respectively.

4.2. Model validation

In the simulation, the initial and boundary conditions are identical to those of the experiment. The physical parameters of the HTF and PCM are listed in Table 5 and Table 6.

Table 5 Physical parameters of PCM

PCM	Phase change temperature (℃)	Density (kg/m^3)	Specific heat capacity [J/(kg·℃)]	Phase change heat (kJ/kg)	Kinematic viscosity (m^2/s)	Thermal conductivity [W/(m·℃)]
Water	0	1000 (l) 916 (s)	4200 (l) 2090 (s)	334	1.732×10^{-6}	0.55 (l) 2.22 (s)

Table 6 Physical parameters of HTF

HTF	Density (kg/m^3)	Thermal conductivity [W/(m·℃)]	Specific heat capacity [J/(kg·℃)]	Kinematic viscosity (m^2/s)
25% glycol	1036	0.45	3.85	1.71×10^{-6}

4.2.1 Validation of the ice storage process

The comparisons of the near inlet temperature of HTF between simulation and experiment during the ice storage process are shown in Fig. 11:

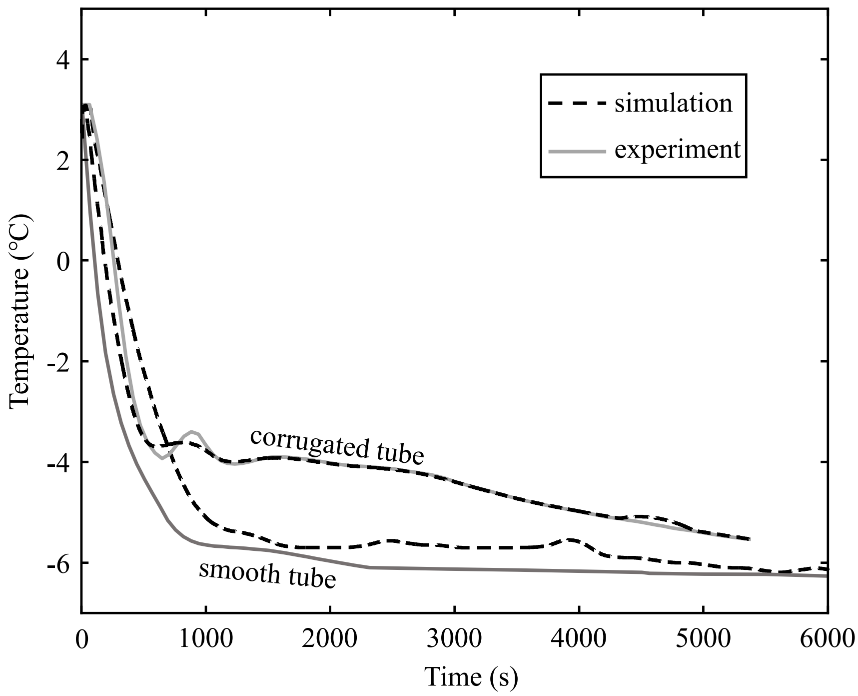

Fig. 11. Comparison of experiment and simulation between smooth-tube and corrugated-tube heat exchanger during the ice storage process

Maximum deviation between simulation results and experimental results is 1.5 °C. The root-mean-square error (RMSE) between the numerical and experimental results of the smooth-tube and corrugated-tube heat exchanger is 0.94 and 0.31 respectively, which meets the accuracy requirements. The result indicates that the simulation temperature of smooth-tube heat exchanger is higher than experimental temperature. This can be attributed to the different convective heat transfer coefficient between the simulation and real experiment. Also, some thermodynamic properties are assumed constant in numerical simulation while they may vary in real experiment.

4.2.2 Validation of the melting process

The comparisons of the near inlet temperature of HTF between simulation and experiment during the melting process are shown in Fig. 12:

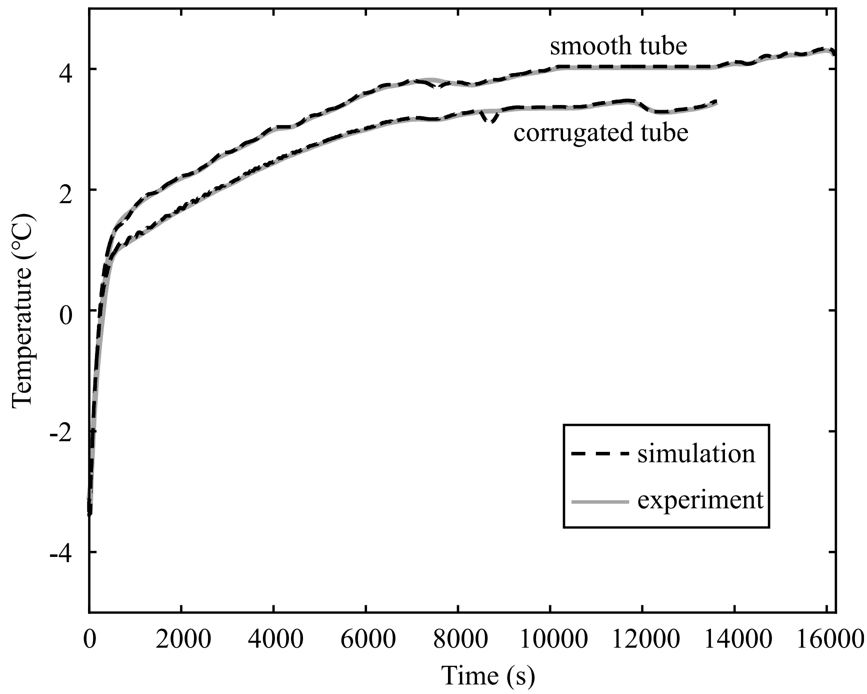

Fig. 12. Comparison of experiment and simulation between smooth-tube and corrugated-tube heat exchanger during the melting process

The curves of the experimental results and the simulation results are similar and consistent and data errors are within 0.5 ℃. The RMSE between the numerical and experimental results of the smooth-tube and corrugated-tube heat exchangers is 0.06 and 0.07 respectively, which meets the accuracy requirements. The agreement demonstrated the feasibility of the present numerical model in the prediction of melting process. In this context, it is reasonable and reliable to investigate the melting performance based on the prediction of the present model.

4.3. Numerical simulation analysis

4.3.1 Ice storage / melting characteristics

Fig. 13 shows the ice mass fraction of PCM along the length of the smooth tube and corrugated tube at different time during the ice storage process. The low-temperature HTF enters from the inlet of the tube, which leads to the phenomenon that the inlet position of the tube is first covered with ice during the ice storage process. Along the axial direction of the tube, the freezing is significantly delayed and the ice layer around the tube is thinner and thinner. Similarly, the PCM around the inlet position of the tube melts firstly. Along the axial direction of the tube, the melting process is also delayed, and the ice outside the end of the tube melts finally.

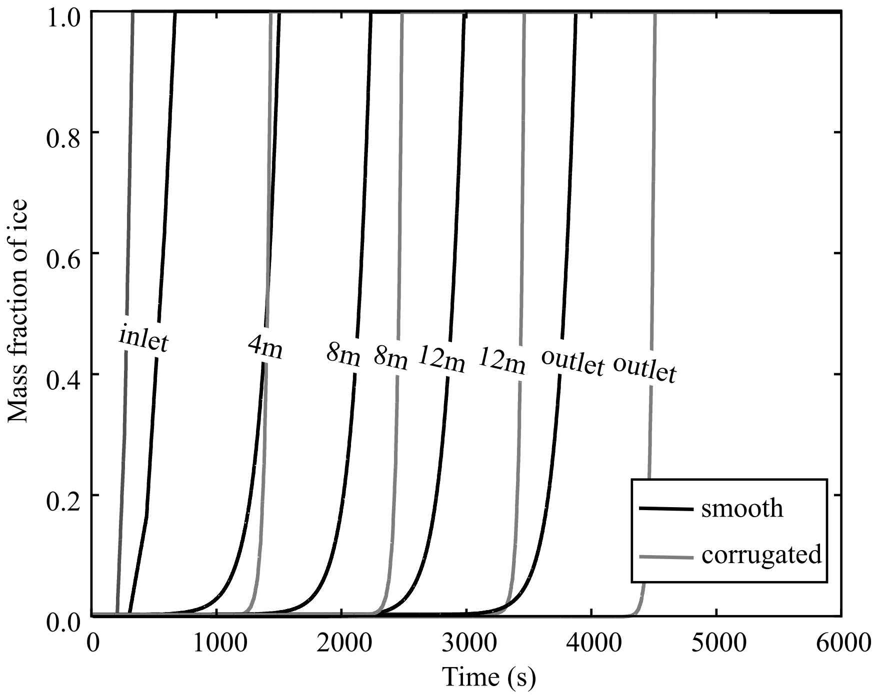

Fig. 13. Ice mass fraction of smooth-tube and corrugated-tube heat exchangers versus time during the ice storage process

It is also seen from Fig. 13 that there is a faster solidification rate of corrugated-tube heat exchanger. The solidification rate of corrugated-tube heat exchanger is about 2.5 times faster than that of the smooth-tube heat exchanger. This indicates that the corrugated-tube heat exchanger has higher heat transfer coefficient in comparison with the smooth-tube heat exchanger.

The ice mass fraction of PCM within smooth-tube heat exchanger and corrugated-tube heat exchanger versus time during the melting process is shown in Fig. 14. The inlet temperature of HTF is higher during the melting process, which leads to that the ice near the inlet of the tube melts firstly. The melting rate of corrugated-tube heat exchanger is about 9 times faster than that of the smooth-tube heat exchanger.

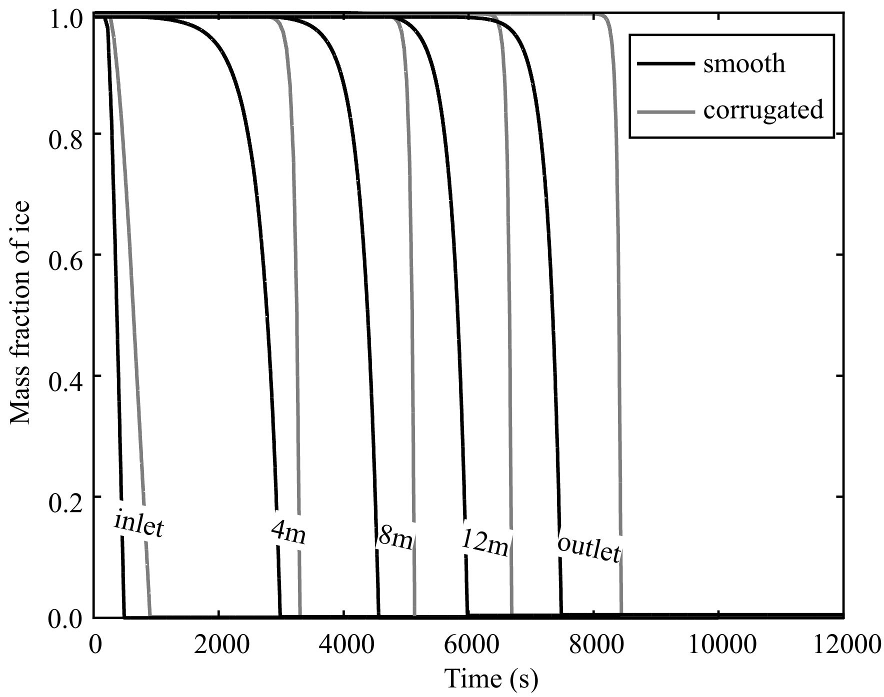

Fig. 14. Ice mass fraction of smooth-tube and corrugated-tube heat exchangers versus time during the melting process

4.3.2 Temperature characteristics

The temperature variation of ice/water with time at different positions of the smooth-tube and corrugated-tube heat exchangers during the ice storage process is shown in Fig. 15 and Fig. 16. At inlet of smooth-tube heat exchanger, the temperature of the water increases from 2 ℃ to 3 ℃, decreases from 3 ℃ to the freezing point during water sensible heat storage period and the phase change process undertakes from 380s to 570s time period. The temperature of the solid ice further drops more quickly to the temperature of -5.6 ℃ at 1620s, then it remains relatively stable. This is because that the initial water temperature in the ice-storage tank is lower than the boundary condition, leading to the small rise of water temperature. While after the phase change process, the sensible heat transfer rate of ice is higher than that of water, which is attributed to that the specific heat of the solid ice is lower than that of the liquid water. At inlet of corrugated-tube heat exchanger, the temperature of the water increases from 2 ℃ to 3 ℃, decreases from 3 ℃ to the freezing point and the phase change process undertakes from 250s to 340s time period. The temperature of the solid ice further drops more quickly to the temperature of -4 ℃ at 650s, then it decreases relatively slowly. There is a temperature fluctuation between 650s and 1000s because of the fluctuation of the HTF temperature at the same time. At outlet of smooth-tube and corrugated-tube heat exchanger, the temperature of the water decreases from 2.5 ℃ to the freezing point and phase change process undertakes from 700s to 3770s and from 550s to 4400s time period, respectively. The temperature of solid ice drops more quickly to the temperature of -5.6 ℃ and -5.2 ℃, respectively.

The maximum effective solidification duration of PCM within the smooth-tube heat exchanger is 3070 s, accounting for 42.7% of the smooth-tube ice-storage duration. While the maximum effective solidification duration of PCM within the corrugated-tube heat exchanger is 3850s, accounting for 71.3% of the corrugated-tube ice-storage duration.

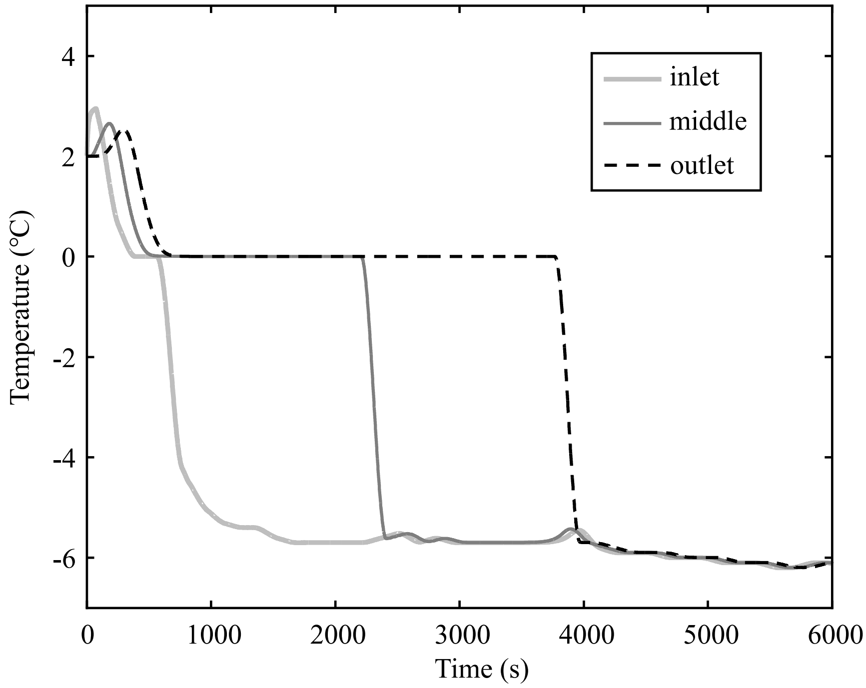

Fig. 15. Temperature variation of the ice/water with time at different positions of smooth-tube heat exchanger during the ice storage process

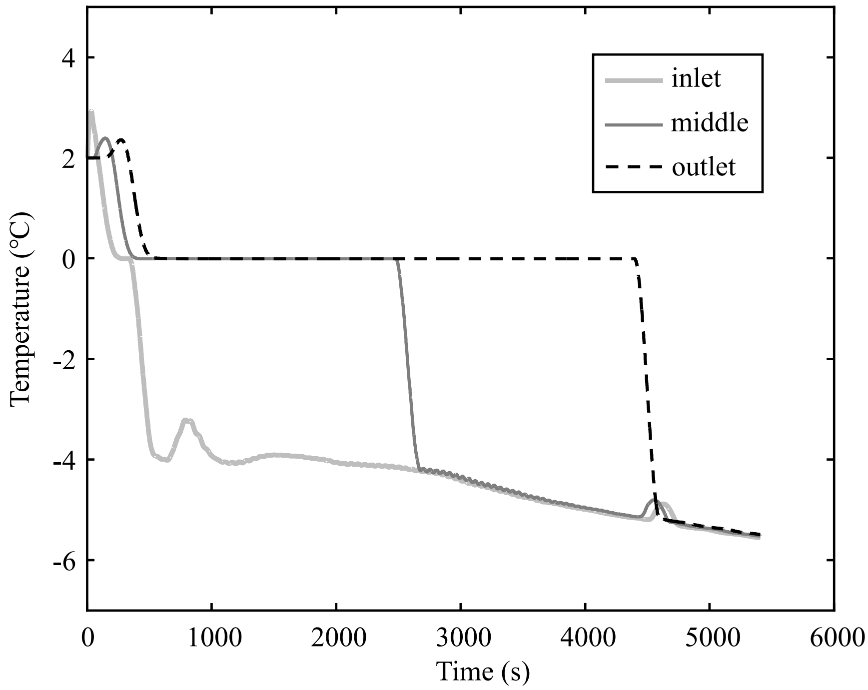

Fig. 16. Temperature variation of the ice/water with time at different positions of corrugated-tube heat exchanger during the ice storage process

Fig. 17 and Fig. 18 depict the temperature variation of ice/water with time at different positions of the smooth-tube and corrugated-tube heat exchangers during the melting process. As it is shown in the Fig. 17, the ice temperature at inlet of the smooth-tube heat exchanger increases from the initial temperature of -3.5 ℃ to the melting point and the phase change process undertakes from 400s to 660s time period. The temperature of the liquid water further rises more slowly to the temperature of 1.65 ℃ at 1100s, then it rises slowly and steadily. At the outlet of the smooth-tube heat exchanger, the temperature of ice increases from the initial temperature of -3.5 ℃ to the melting point and the phase change process undertakes from 600s to 7300s time period. The temperature of water further rises more slowly to the temperature of 3.8 ℃ at 7800s, then it does not change significantly. As it is shown in the Fig. 18, the ice temperature at outlet of the corrugated-tube heat exchanger increases from the initial temperature of -3.5 °C to the melting point and the phase change process undertakes from 500s to 8200s time period. The temperature of the liquid water further rises more slowly to the temperature of 3.3 °C at 8700s, then it remains relatively stable.

The maximum effective melting duration of PCM within the smooth-tube heat exchanger is 6700 s, accounting for 41.5% of the smooth-tube melting duration. While the maximum effective melting duration of PCM within the corrugated-tube heat exchanger is 7700s, accounting for 56.8% of the corrugated-tube melting duration.

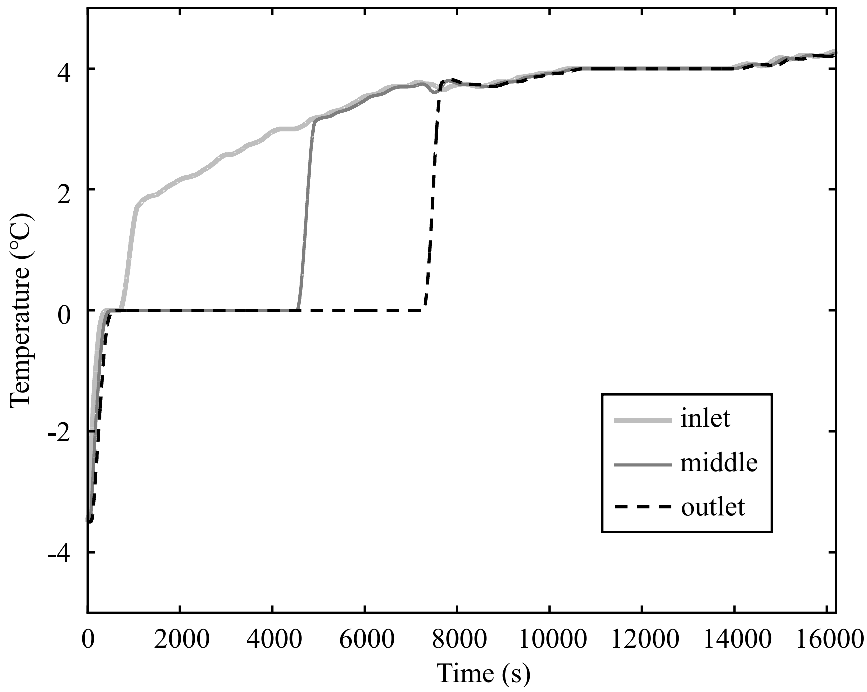

Fig. 17. Temperature variation of the ice/water with time at different positions of smooth-tube heat exchanger during the melting process

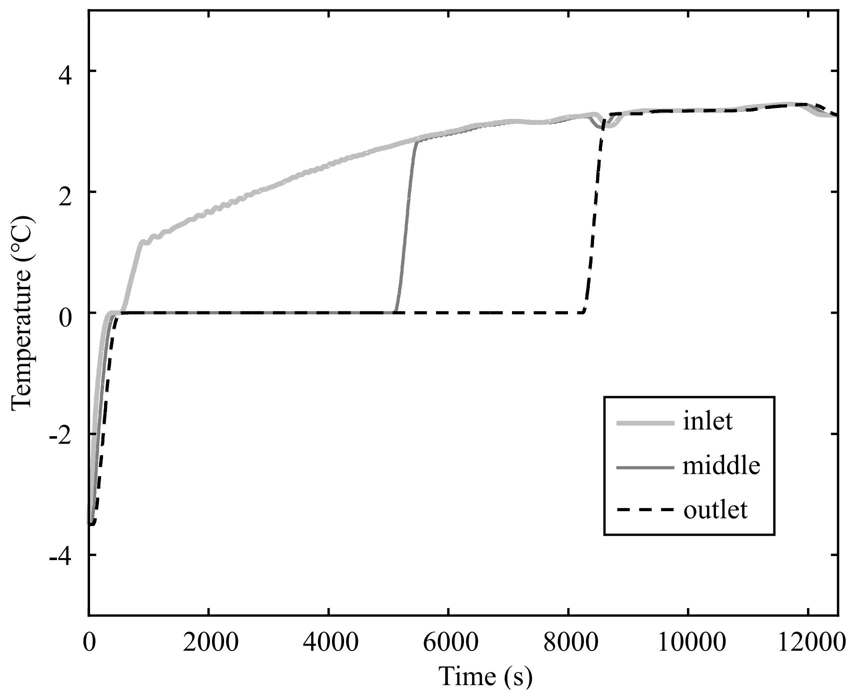

Fig. 18. Temperature variation of the ice/water with time at different positions of corrugated-tube heat exchanger during the melting process

5. Conclusions

In this study, a fast numerical simulation is used to simplify and analyze the ice thermal storage system with smooth-tube heat exchanger and corrugated-tube heat exchanger. The performances of smooth-tube heat exchanger and corrugated-tube heat exchanger for ice storage and melting are compared by experiment and numerical simulation. The conclusions are drawn as follow:

(1) The simulation results are basically consistent with the experimental results. The root-mean-square error between the numerical and experimental results of smooth-tube and corrugated-tube heat exchanger is 0.94 and 0.31 during the ice storage process, as well as 0.06 and 0.07 during the melting process. This is validated for the numerical model during ice storage and melting process. It is reasonable and

reliable to investigate ice-storage and melting performances based on the prediction of the model.

(2) Under the same conditions, the ice-storage duration and melting duration of the corrugated-tube heat exchanger is shortened by 25% and 16% compared with those of the smooth-tube heat exchanger.

(3) During the ice storage process, the temperature difference between the inlet and outlet of the corrugated tubes is 0.4 °C less than that of the smooth tubes. During the melting process, the temperature difference between the inlet and outlet of the corrugated-tube heat exchanger is 0.1 °C larger than that of the smooth-tube heat exchanger.

(4) During the ice storage process, the heat exchange rate of the corrugated-tube heat exchanger is 2.5 times faster than that of the smooth-tube heat exchanger. During the melting process, the heat exchange rate of the corrugated-tube heat exchanger is 9 times faster than that of the smooth-tube heat exchanger. The heat transfer performances of corrugated tubes are superior.

Acknowledgement

This work was supported by the National Key R&D Program of China (No. 2020YFD1100305-02).

References

[1] Z. Kang, R. Wang, X. Zhou, G. Feng. Research Status of Ice-storage Air-conditioning System. Procedia Engineering, 205 (2017) 1741-1747.

[2] Y. Cao, Y. Jiang, B. Song, S. Jiang, L. Yu. Numerical Simulation and Experiment Study on Dynamic Freezing Characteristics of Ice-on-Coil. Journal of Nanjing University of Aeronautics & Astronautics, 39 (6) (2007) 756-760 [In Chinese].

[3] H. Zhou, M. Chen, X. Han, P. Cao, F. Yao, L. Wu. Enhancement Study of Ice Storage Performance in Circular Tank with Finned Tube. Processes, 7 (5) (2019) 266.

[4] T. Asaoka, Y. Endo. Experimental study on absorption ice slurry generator with ethanol solution as the refrigerant. International Journal of Heat and Mass Transfer, 162 (2020) 120333.

[5]López-Navarro A., Biosca-Taronger J., Torregrosa-Jaime B., Martínez-Galván I., Corberán J.M ., Esteban-Matías J., Paya J. Experimental investigation of the temperatures and performance of a commercial ice-storage tank. International Journal of Refrigeration, 36 (4) (2013) 1310-1318.

[6] Z. Deng, X. Liu, C. Zhang, Y. Huang, Y. Chen. Melting behaviors of PCM in porous metal foam characterized by fractal geometry. International Journal of Heat and Mass Transfer, 113 (2017) 1031-1042.

[7] J. Wang, L. Sun, M. Zou, W. Gao, C. Liu, L. Shang, Z. Gu, Y. Zhao. Bioinspired shape-memory graphene filmwith tunable wettability. Science Advances, 3 (6) (2017) Article e1700004.

[8] R.L.Webb, Wiley. Principles of enhanced heat transfer. Great Britain, Chemical Engineering Science. 50 (18) (1995) 3007.

[9] K. Navickaitė, L. Cattani, C.R.H. Bahl, K. Engelbrecht. Elliptical double corrugated tubes for enhanced heat transfer. International Journal of Heat and Mass Transfer, 128 (2019) 363-377.

[10] Y. Huang, Q. Sun, F. Yao, C. Zhang. Performance optimization of a finned shell-and-tube ice storage unit. Applied Thermal Engineering, 25 (2020) Article 114788.

[11] Hani Hussain Sait. Design and analysis of a flooded tube for cold energy storage. International Journal of Refrigeration, 94 (2018) 151-160.

[12] X. Jia, X. Zhai, X. Cheng. Thermal performance analysis and optimization of a spherical PCM capsule with pin-fins for cold storage. Applied Thermal Engineering, 148 (2019) 929-938.

[13] J. Yang, L. Yang, C. Xu, X. Du. Experimental study on enhancement of thermal energy storage with phase-change material. Applied Energy, 169 (2016) 164-176.

[14] C. Yu, Q. Peng, X. Liu, P. Cao, F. Yao. Role of metal foam on ice storage performance for a cold thermal energy storage (CTES) system. Journal of Energy Storage, 28 (2020) Article 101201.

[15] Changfa Ji. Influence of geometric parameters of fin on ice storage of tube with inner fin. Journal of Liaoning Technical University, 24 (2005) 267-269 [In Chinese].

[16] S. Arena, E. Casti, J. Gasia, L.F. Cabeza, G. Cau. Numerical analysis of a latent heat thermal energy storage system under partial load operating conditions. Renewable Energy, 128 (2018) 350-361.

[17] N.R.Vyshak, G.Jilani. Numerical analysis of latent heat thermal energy storage system. Energy Conversion and Management, 48 (7) (2007) 2161-2168.

[18] J. Xu, X. Wang. Numerical simulation of fluid flow and transfer in corrugated tubes. Petro-Chemical Equipment, 37 (1) (2008) 4-7 [In Chinese].

[19] Manhe Du. Corrugated tube heat exchanger. Chemical Equipment Technology, 21 (2000) 42-44 [In Chinese].

[20] Q. Hu, X. Qu, W. Pen, J. Wang. Experimental and numerical investigation of turbulent heat transfer enhancement of an intermediate heat exchanger using corrugated tubes. International Journal of Heat and Mass Transfer, 185 (2022) Article 122385.

[21] Y. Zhang, S. Zhang, D. Wang, Y. Liu, H. Deng, B. Hu, M. Tang. Flow behavior of liquid falling film on a horizontal corrugated tube. Annals of Nuclear Energy, 148 (2020) Article 107728.

[22] D. Yang, H. Li, T. Chen. Pressure drop, heat transfer and performance of single-phase turbulent flow in spirally corrugated tubes. Experimental Thermal and Fluid Science, 24 (2001) 131-138.

[23] P. Yang, H. Zhang, Y. Zheng, Z. Fang, X. Shi, Y. Liu. Investigation and optimization of heat transfer performance of a spirally corrugated tube using the Taguchi method. International Communications in Heat and Mass Transfer,127 (2021) Article 105577.

[24] J.I.Corcoles, J.D.Moya-Rico, A.E.Molina, J.A.Almendros-Ibanez. Numerical and experimental study of the heat transfer process in a double pipe heat exchanger with inner corrugated tubes. International Journal of Thermal Sciences, 158 (2020) Article 106526.

[25] X. Chen, H. Han, K.S. Lee, B. Li, Y. Zhang. Turbulent heat transfer enhancement in a heat exchanger using asymmetrical outward convex corrugated tubes. Nuclear Engineering and Design, 350 (2019) 78-89.

[26] A.López-Navarro, J. Biosca-Taronger, B. Torregrosa-Jaime, J.M. Corberán, J.L. Bote-García, J. Payá. Experimental investigations on the influence of ice floating in an internal melt ice-on-coil tank. Energy and Buildings, 57 (2013) 20-25.

[27] Wenquan Tao, Numerical Heat Transfer (Second Edition). Xi'an Jiaotong University Travel Agency, (2001) 4-5 [In Chinese].

[28] Son C H, Morehouse J H. Thermal conductivity enhancement of soild -soild phase change materials for thermla storage. Journal of thermophysics and heat transfer, 5 (1991) 122-124.

[29] Kui Lang. Design of corrugated tube heat exchanger. Energy conservation, 6 (1995) 38-41.

[30] Von Volker Gnielinski, Forschung im Lngenieurwesen, Band. 41(1975).